Covalent linkages of molecules and proteins to Si−H surfaces formed by disulfide reduction

Essam M. Dief [1], Yan B. Vogel[1], Chandramalika R. Peiris[1], Anton P. Le Brun[2], Vinicius R. Gonçales[3], Simone Ciampi[1], Jeffrey R. Reimers[4,5] and Nadim Darwish[1]*

[1]School of Molecular and Life Sciences, Curtin Institute of Functional molecules and Interfaces, Curtin University, Bentley, WA 6102, Australia

[2]Australian Centre for Neutron Scattering, Australian Nuclear Science and Technology Organization (ANSTO), Lucas Heights, NSW 2234, Australia

[3]School of Chemistry, Australia Centre for NanoMedicine, ARC Centre of Excellence in Convergent Bio-Nano Science and Technology, University of New South Wales, Sydney, NSW 2052, Australia

[4]International Centre for Quantum and Molecular Structures, School of Physics, Shanghai University, Shanghai 200444, China

[5]University of Technology Sydney, School of Mathematical and Physical Sciences, Ultimo, New South Wales 2007, Australia

ABSTRACT: Thiols and disulfides contacts have been, for decades, key for connecting organic molecules to surfaces and nanoclusters as they form self-assembled monolayers (SAMs) on metals such as gold (Au) under mild conditions. In contrast, they have not been similarly deployed on Si owing to the harsh conditions required for monolayers formation. Here, we show that SAMs can be simply formed by dipping Si−H surfaces into dilute solutions of organic molecules or proteins comprising disulfide bonds. We demonstrate that S−S bonds can be spontaneously reduced on Si−H, forming covalent Si−S bonds in the presence of traces of water, and that this grafting can be catalyzed by electrochemical potential. Cyclic disulfide can be spontaneously reduced to form complete monolayers in 1 hour and the reduction can be catalyzed electrochemically to form full surface coverages within 15 minutes. In contrast, the kinetics of SAM formation of the cyclic disulfide molecule on Au was found to be three folds slower than that on Si. It is also demonstrated that dilute thiol solutions can form monolayers on Si−H following oxidation to disulfides under ambient conditions; the supply of too much oxygen, however, inhibits SAM formation. The electron-transfer kinetics of the Si–S enabled SAMs on Si–H is comparable to that on Au SAMs, suggesting that Si−S contacts are electrically transmissive. We further demonstrate the prospective of this spontaneous disulfide reduction by forming a monolayer of protein azurin on a Si–H surface within 1 hour. The direct reduction of disulfides on Si electrodes opens new capabilities for a range of fields, including molecular electronics, for which highly conducting SAM–electrode contacts are necessary, and for emerging fields such as bio-molecular electronics as disulfide linkages could be exploited to wire proteins between Si electrodes, within context of the current Si-based technologies.

1. INTRODUCTION

Silicon-based technology has been the corner stone of the electronics industries, owing to its fabrication feasibility, low cost and abundance in nature.[1-3] Parallel to this progress, molecular electronics has been developed and it is anticipated that future electronics will involve the use of molecules as active components. The development of molecular and Si electronics technologies suggest that the time has come to integrate the electrical properties of semiconductors with the chemical diversity of organic molecules to unlock powerful and miniaturized electronic components.[4-8] The outcomes have the potential to revolutionize the Si-based electronics sector, through creating unprecedented capacity for miniaturization and integration of new device properties – the properties of organic molecules.

One of the challenges in Si-based molecular electronics is that the naturally grown oxide layer on the surface of crystalline Si produces insulating properties that shadow its semiconducting

properties.[9, 10] Therefore, Si wafers require etching of the native oxide layer to expose conductive Si−H surfaces, which then must be protected by chemical modification to prevent re-oxidation.[4, 11] Such processing is intrinsically more complicated than thin film modification of metal surfaces such as Au, processes that have dominated the field of molecular electronics[12-14] and many other applications.[15-19] Although the formation of thiol-based self-assembled monolayers (SAMs) on Au is simple and involves spontaneous self-assembly,[20, 21, 22] these monolayers show limited mechanical stability and can adopt a very wide range of structural motifs owing to the dominant van der Waals characteristics of surface Au−S bonding.[23-28]

Formation of SAMs on Si−H surfaces utilizing Si−C bonding is established as an alternative that can deliver chemically and thermally stable organic molecular films.[11, 29-32] Most hydrosilylation protocols for the formation of covalent Si−C bonding on Si−H require a radical initiators obtained using UV radiation,[33, 34] visible light,[35] heat,[36-38] or chemical reagents.[36, 39-41]

Alkyl thiol monolayers have been assembled on Si−H only with the assistance of external stimuli such as UV light[46,32] or by implementing a tailored experimental set-ups such as using ultra-high vacuum[33] or continuous flow of supercritical carbon dioxide(SCCO$_2$).[34] The mechanism of forming sulfur-based SAMs on Si−H has been demonstrated to involve a radical chain reaction. Buriak et al[47] demonstrated that a radical initiator such as diazonium salts is required to generate a silyl radical Si$^•$ that initiates a radical chain reaction forming a Si−S based SAM. Also, Sugimura and co-workers[48] have shown that Si(111)−H surface heated in a high boiling point solvent resulted in forming a Si−S bonded SAMs through initiating Si$^•$ radicals on Si−H surface and propagating thorough a radical chain. In a previous report, we demonstrated that solutions of straight-chain alkyl thiols, exposed to air during the grafting, forms dense monolayers on Si.[49] These results were interpreted in terms of the reaction of thiols RSH with dissolved oxygen to form disulfides (RSSR) that would be in equilibrium with trace amounts of thiyl radicals (RS$^•$) in solution. Calculations using density functional theory (DFT) were used to predict that the thiyl radical intermediates could barrierlessly abstract a Si−H hydrogen to form a surface radical that could then participate in a free-radical polymerization reaction with solution alkyl thiols to form SAMs under ambient conditions.

Previous investigations of the reduction of disulfides in solution demonstrated that cyclic disulfides are highly prone to reduction, and thus they are easily reduced in solution as compared to linear disulfides.[50]

These properties established five-membered ring disulfides, such as alpha lipoic acid, as antioxidants and radical scavengers in biological systems.[51, 52]

In this work, we investigate the reaction of Si−H with disulfides to form SAMs, and the dependence of conversion of the linear alkyl thiol into disulfides on oxygen exposure, with controlled oxygen being reasoned to lead to significant conversion of thiol to disulfide in solution – can disulfides react directly to contribute to SAM formation? We also ask the question as to whether proteins comprising disulfide bonds can be covalently connected to Si electrodes spontaneously. Returning to the gold analogy, we note that disulfides also form SAMs on Au, first through strong physisorption and then by chemisorption following S–S homolytic bond cleavage,[9, 24, 53-57] both under ambient conditions[58, 59] and under electrochemical control.[60] It is mostly agreed that disulfides are physisorbed first then undergo hemolytic cleavage on Au surfaces forming Au−S bonds.[61] However on Si, there is no evidence of strong physisorption of sulfur containing compounds.

Here, we demonstrate the formation of monolayers using disulfide containing molecules (**1** and **2**) utilizing 1,2-dithiolane-3-pentanoic acid (known as alpha lipoic acid), see Figure 1. We assess the kinetics of the spontaneous reduction of the disulfide bond and investigate the reaction catalysis electrochemically. We further demonstrate that alkyl thiols (**3**) that are first converted to disulfides, can form SAMs on Si−H significantly faster than freshly prepared solutions. In addition, we investigate the experimental conditions needed to convert thiols to disulfides to facilitate a rapid SAM formation on Si−H and investigate the covalent attachment of the protein azurin (**4**) via its sulfide moieties. The SAMs are characterized by X-ray photoelectron spectroscopy (XPS), X-ray reflectometry (XRR) and atomic force microscopy (AFM) to determine the structure of the monolayers, and electrochemically to determine the electron transfer kinetics and the molecular coverages on both Si and Au electrodes.
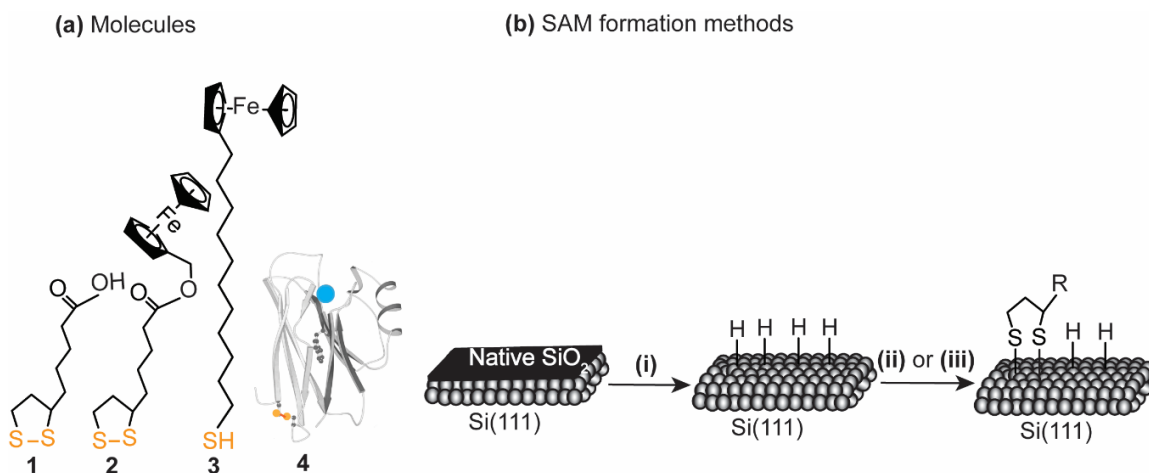

Figure 1. (a) Structures of the molecules studied. (b) Schematic illustration of the grafting process on Si(111)−H electrodes. (i) Cleaning Si wafers with piranha solution (3:1 (v:v)) mixture of concentrated sulfuric acid and 30% hydrogen peroxide, respectively), then etched with 40% NH$_4$F to form Si−H surfaces. Molecules **1-4** are grafted by spontaneous (ii) or electrochemical grafting (iii). **4** represents the protein azurin with a disulfide (yellow dots) at one end and the copper centre (blue dot) impeded inside the protein matrix at the opposite end.

2. MATERIALS AND METHODS

2.1 Chemicals and Reagents. All chemicals used were of analytical grade from Sigma Aldrich, unless otherwise stated, and were used without any further purification. Sulfuric acid (Puranal TM, 95−97%), hydrogen peroxide (30 wt. % in water) used piranha treatments step were of semiconductor grades from Sigma Aldrich. Ammonium fluoride (Puranal TM, 40 wt. % in water) used in Si etching step was bought from Sigma Aldrich as well. (±)-α-Lipoic acid ≥ 98.0 %, ferrocenemethanol 97%, N,N′-dicyclohexycarbodiimide (DCC) 99% and N,N-dimethylpyridin-4-amine (DMAP) ≥ 99% were obtained from Sigma Aldrich and used as received. The dichloromethane (DCM), acetonitrile (ACN), isopropyl alcohol, and ethanol solvents were purified by distillation before use. Glacial acetic acid, ≥ 99.85 %, used in preparing the SAMs, was purchased from Sigma Aldrich. Silicon wafers were purchased from Siltronix, S.A.S. (Archamps, France). The P-type silicon was boron highly doped, with resistivity ca. 0.007 Ω cm or 10 Ω cm (for low doped), and wafer thickness of 500 ± 25 μm oriented ± 0.5° away from (111) plane. N-type silicon was phosphorous doped with resistivity of 0.001 Ω cm (for highly doped). Tetrabutylammonium hexafluorophosphate 98%, used in electrochemical reduction, was purchased from Sigma Aldrich. Milli-Q water (>18 MΩ cm) was used for all the cleaning procedures and the electrolytes preparation. The protein azurin from Pseudomonas aeruginosa, lyophilized powder, was bought from Sigma Aldrich.

2.2 Chemical synthesis of 2. Molecule **2** was synthesized using DCC/DMAP coupling, using a reaction adopted from Limoges and co-workers.[62] Briefly, to a solution of (±)-α-Lipoic acid (247 mg, 1 mmol) in dry CH_2Cl_2 (40 mL) was added ferrocenemethanol (216 mg, 1.2 mmol) and DMAP (40 mg, 0.35 mmol). The mixture was then stirred at room temperature for 30 min and then cooled down to 0 °C. A solution of N,N′-dicyclohexycarbodiimide (DCC) (0.226 mg, 1.2 mmol) in CH_2Cl_2 was then slowly added. The solution was stirred at room temperature for 24 h. The organic phase was then filtered, dried in a rotary evaporator, and the crude product was purified using hexane: ethyl acetate (8:2) solvent mixture running through a silica gel column. The retention factor (Rf) of ferrocenemethanol (on silica TLC) was about 0.1, the alpha lipoic acid, **1**, stays at the baseline, and the product moves with an Rf of ~0.7.

2.3 Preparation of Si−H electrodes and disulfide molecules SAMs. Si electrodes were prepared by cutting the wafers into pieces (approximately 1×1 cm²), then treated with piranha solution (a 3:1 (v:v)) mixture of concentrated sulfuric acid and 30% hydrogen peroxide, respectively) at 130 ºC for 30 minutes. After piranha cleaning, the Si electrodes were rinsed with water and etched with a deoxygenated 40% aqueous ammonium fluoride solution, containing traces of sodium sulphite scavenger, for 13 minutes. For spontaneous grafting, the freshly etched Si−H electrodes were dipped in a 5 mM solution of **1, 2** or **3** dissolved in acetonitrile (ACN) for 1 hour to allow spontaneous formation of the SAMs (Note: **3** was prepared then left for 24 hours at ambient conditions before grafting). For electrochemical grafting, 5 mM of **1** or **2** was dissolved in ACN containing 0.1 M tetrabutylammonium hexafluorophosphate (NBu₄ PF₆) . A potential of −0.8 V versus an Ag/AgCl reference electrode was then applied, for 15 minutes, to the Si−H electrode as the working electrode, immersed in ACN solution containing the electrolyte salt (NBu₄ PF₆) . After either spontaneous or electrochemical SAM grafting, the electrodes were washed using

DCM, followed by drying under a stream of Ar gas before further analysis.

2.4 Preparation of azurin protein monolayer on Si. The freshly etched Si−H surface was covered with a droplet of 100 mM ammonium acetate of pH 4.6 containing the protein azurin (200 pM) for 1 hour, then washed thoroughly with the buffer solution and water before measurement.

2.5 Electrochemical Measurements. All electrochemical measurements were performed with a CHI650 (CH Instruments, USA) electrochemical workstation, using a conventional three-electrode system. Cyclic voltammetry measurements and square wave voltammetry were carried out in 1 M $NaClO_4$ solution.

2.6 Atomic Force Microscopy imaging. AFM topography images were acquired using a Bruker dimension microscope, operating in tapping mode. All images were recorded using silicon nitride cantilevers (TESPA from Bruker, with a spring constant of 20 N m–1) at room temperature, in air.

2.7 X-ray photoelectron spectroscopy (XPS) analysis. XPS measurements were performed on a Kratos Axis Ultra DLD spectrometer, using a monochromatic Al-Kα (1486.6 eV) irradiation source operating at 150 W. Spectra of Si 2p (90–110 eV), C 1s (277–300 eV), and S 2p (163−164 eV) were taken in normal emission at or below 7×10–9 Torr. Data files were processed using CasaXPS© software, and the reported XPS energies are binding energies expressed in eV. After background subtraction (Shirley), spectra were fitted with Voigt functions. To correct for energy shifts caused by adventitious charging, all peak energies were corrected with a rigid shift to bring the C 1s emission to 284.8 eV.

2.8 XRR analysis. A Panalytical Ltd X′Pert Pro was used to record X-ray reflectometry (XRR) at the solid-air interface with a tube source (Cu Kα radiation, λ = 1.54 Å). The X-ray beam was focused using a Göbel mirror and collimated using fixed slits of 0.1 mm.

3. RESULTS AND DISCUSSION

As detailed, in Methods, SAMs of **1–4** on p-type highly doped Si(111)−H are produced and characterized. Two different formation processes are used for **1** and **2** from acetonitrile solution: spontaneous grafting achieved at open circuit potential in ambient conditions, and electrochemical grafting achieved by applying an electrochemical potential, which catalyzed the reaction enabling the SAM formation to proceed to completion in a relatively shorter time. SAMs of **3** are grown, after air exposure for 24 hours, spontaneously similar to **2**.

3.1 Si−S covalent bonding. Detailed XPS characterization was performed to determine the chemical bonding of the Si−S-based monolayers on Si electrodes. The results indicate that SAMs of **1** and **2** on Si−H were successfully formed. Figure 2 shows results obtained for SAMs of **1** formed spontaneously under ambient conditions. The survey spectrum shown in Figure 2a indicates the presence of the atomic components of **1**: C, S and O atoms. Elemental analysis for the XPS survey spectrum (Figure 2a inset) shows that the atomic ratios C: O is 4:1, reflecting comparable theoretical elemental compositions of molecule **1** ($C_8H_{14}O_2S_2$). The S 2p spectral envelope can be fitted in terms of three components, as shown in Figure 2b. Two components, centred at 163.1 eV and 164.28 eV, have an apparent 2:1 height ratio, similar width, and a splitting of 1.18 eV, consistent[63] with
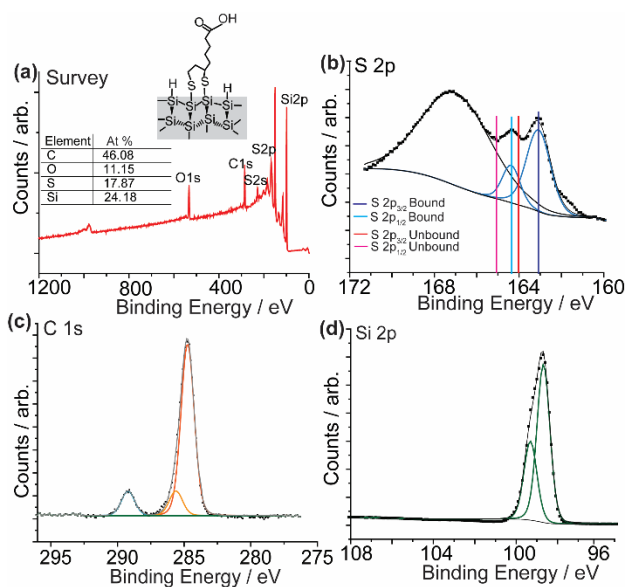
Figure 2. XPS analysis for a SAM of 1 formed by spontaneous grafting on p-type highly doped Si(111)−H. a) Survey spectrum showing the elemental analysis of the SAM on the Si surface, reflecting the C, S and O atomic ratios as expected from the chemical composition of molecule 1 (Inset table). b) S 2p envelope, with an emission between 161 and 166 eV characteristic of covalent Si−S bonding, with the doublet centred at 163.1 eV assigned to the bound thiolate (marked with blue lines) and the red marks labelling the expected position for the unbound disulfides. c) C 1s emission between 284 and 290 eV, with C atoms in three different environments, with the peak at 284.8 eV corresponding to C−C/C−S bonding, the peak at 285.7 eV assigned to the particular carbon adjacent to the COOH group, and the peak centred at 289.3 eV assigned to the COOH carbon, indicating the presence of all the components of 1, C, S, and O in the formed monolayer. d) Si 2p emission between 99.3−106.0 eV, with the absence of peaks around 103.5 eV, indicating that no detectable oxide is present on Si−H functionalized surface and the SAM is well protecting the Si.

expectations for the S $2p_{3/2}$ and S $2p_{1/2}$ orbitals, under the conditions of Si−S covalent bonding, respectively. The broad peak at 168 eV is assigned to the Si plasmon loss that results from strong interactions between Si-surface electrons and the emitted photoelectron.[64, 65] From the observed spectra, there is no evidence to suggest that the two S atoms on the adsorbate molecule are in different chemical environments, and hence it is most likely that both sulfurs bind to the Si surface, similar to that observed for thiol SAMs on copper which have similar electronegativity to Si,[66, 67] with no evidence for a free thiol or unbound disulfide, that have a slightly higher binding energy (position marked in figure 2b).[68]

Shown in Figure 2c, emission in the C 1s region indicates that carbon atoms have three different chemical environments. The largest resolved peak centred at 284.8 eV is assigned to carbon atoms with only single bonds to C or S atoms. From amongst this band can be seen a peak centred at ca. 285.7 eV. This is assigned to the particular carbon adjacent to the COOH group. In addition, a small but well-resolved band centred at 289.3 eV is observed and assigned to the COOH carbon.

In Figure 2d, high-resolution Si 2p spectra reveal one asymmetric band centered at 99.4 eV that is deconvoluted into two

components. These components are separated in energy by 0.63 eV, have similar widths and an area ratio of 2:1, and are assigned to be Si $2p_{3/2}$ and $2p_{1/2}$ spin orbital split. Of most significance, no signal is observed in the 103−106 eV region, indicating that no detectable silicon oxides are present.

XPS spectra obtained following electrochemical grafting of 1 and the spontaneous grafting of 2 to Si(111)−H (Figure S1-S2) show similar chemical bonding to that detailed above following spontaneous of a SAM of 1 under ambient conditions, indicating that the monolayer obtained from different preparation methods have the same chemical bonding. In addition, the presence of the Fe 2p signal and the S 2s signal of 2 on Si confirming the covalent bonding of 2 to Si (Figure S2).

3.2 Disulfide reaction to produce smooth SAMs on Si. Figure 3a shows AFM topography imaging of Si electrodes functionalized with SAMs of 1 made by spontaneous grafting on p-type highly doped Si(111); related images scanned over larger areas of different regions are shown in supporting information (Figure S3). The results depict large flat terraces with smooth atomic edges, with peak-to-peak surface roughness within individual terrace of ca. 0.24 nm, consistent with other alkyl chain SAMs on Si–H.[69] Such small surface roughness indicates the formation of monolayers that are smooth on the length scale of the AFM tip. Results obtained for electrochemically grafted SAMs of 1 shown in Figure 3b are similar to those obtained from the spontaneously formed SAMs, with a relatively lower roughness of ca. 0.2 nm. Nanoscale oxidation appearing as white spots where visible on the Si surface for both methods, and is more pronounced for the spontaneously prepared samples. The thickness of the SAM of 1 on Si−H surface is ~1 nm using XRR measurements (Table S1), consistent with the theoretical length of 1 (Figure 3c).

Figure 3d shows Si 2p XPS spectra of SAMs formed from 1 on both n-type highly doped Si(111) and p-type highly doped Si(111)−H, formed by both spontaneous and electrochemical grafting methods, with no detectable oxide signal, a feature attributed to the amount of oxide present being too small to be detected by XPS, a notation that should be taken into account in the Si-based molecular electronics. Only significant amounts of oxides that are observed in AFM images can be detected by XPS.[70]

3.3 Spontaneous versus electrochemical grafting of disulfides to Si. In order to electrochemically assess the formation of SAMs, 2, which has a distal ferrocene moiety, was synthesized according to previously reported procedures[62, 71] with slight modifications, detailed in Methods, with NMR analysis shown in Figure S4 and Figure S5. Figure 4a and Figure 4b show cyclic voltammograms (CVs) at the same scan rate (1 Vs^{-1}), for SAMs produced from 2 in solution by spontaneous grafting for 1 hour, and electrochemical reduction for 15 minutes, respectively. The surface coverage has been controlled by time in the spontaneous grafting (Figure 4d) and controlled by both time and applied potential in electrochemical reduction (Figure 4e).

Spontaneous grafting of 2 in dry solvents showed significantly less surface coverage as compared to grafting in wet solvents (Figure S6). Although the mechanism remains unclear, the spontaneous grafting can be attributed to several factors including nanoscale oxidation of the Si surface by traces of water present in the grafting solvent.[72] Electrons released from the silicon can break the disulfide bonds into a thiyl radical (RS•) and a thiolate anion (RS⁻)[73] which can then react with the Si surface
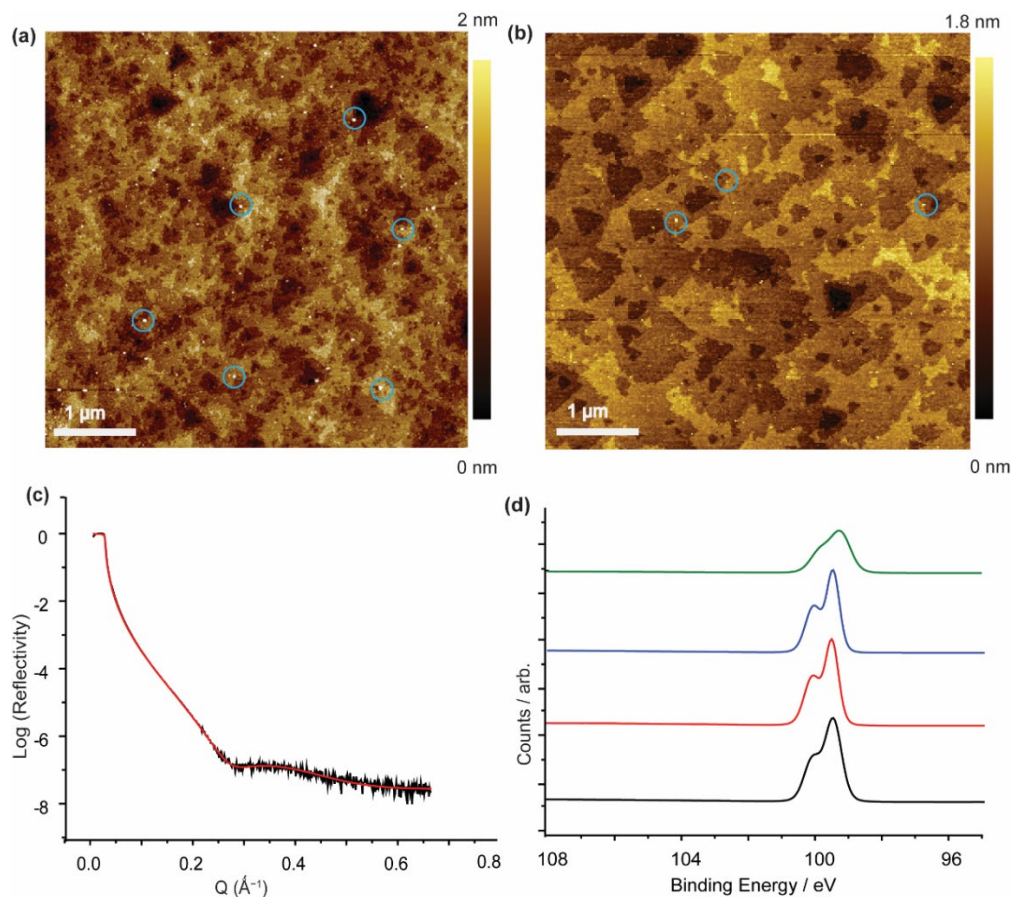
Figure 3. (a) and (b) are AFM topography images of **1** grafted to p-type highly doped Si(111)−H by spontaneous and electrochemical grafting, respectively. (c) XRR spectrum for **1** on p-type highly doped Si(111)−H, raw data (black line) and logarithmic fitting (red line). (d) XPS spectra of Si 2p emission for a SAM of **1** on p-type Si(111)−H spontaneously grafted (black), p-type Si(111)−H grafted electrochemically (red), n-type Si(111)−H grafted spontaneously (blue) and n-type Si(111)−H grafted electrochemically (green). Si etching terraces are clearly visible indicating a smooth SAM formation, with limited surface oxide appearing as white spots, in both spontaneous and electrochemical grafting methods, marked with blue circles as shown in (a) and (b).

to form a SAM (Figure S7). An alternative explanation is water catalyzing the reaction by interfering directly with the primary transition state of the direct reaction of disulfides with Si−H. In parallel to the suggested mechanism above, an oxygen-facilitated radical chemistry can also be a contributor in the grafting process,[49] however this mechanism can not exclusively explain the surface coverage dependence on the water content.

Figure 4c shows the evolution of the current density as a function of the grafting time at applied potentials of −0.8V (black

Further, the open circuit potential (OCP) for the reduction process of **2** in organic electrolyte (0.1 M NB₄uPF₆ in acetoni-

line) and −0.9V (orange line), indicating that more negative potential produces more reductive current, and consequently a higher surface coverage in the voltammetric waves (Figure 4f).

trile) is measured and was found to range from −0.7 V and −

0.65 V, while the OCP for Si−H electrode in the same electrolyte only, ranges from −0.73V to −0.7V (Figure S8).

The shift in OCP toward more positive values in the presence of **2** can be explained by the formation of a more corrosion resistant surface upon the formation of a monolayer. The surface becomes passive with no further shift in the OCP once the SAM is formed and the occupation of the Si surface by the formed monolayer stops the Si from further oxidation, consistent with OCP measurements of monolayer formation on carbon electrodes.[74-76] The OCP analysis is further supported by experiments showing that, applying potentials more positive than the OCP do not accelerate the grafting reaction, by showing similar surface coverage at two different potentials, −0.1 V and −0.4 V (Figure S9). At these potentials the SAM formation happens spontaneously.

Table 1. Values of surface coverage (Γ) calculated from cyclic voltammetry for both Au and Si.

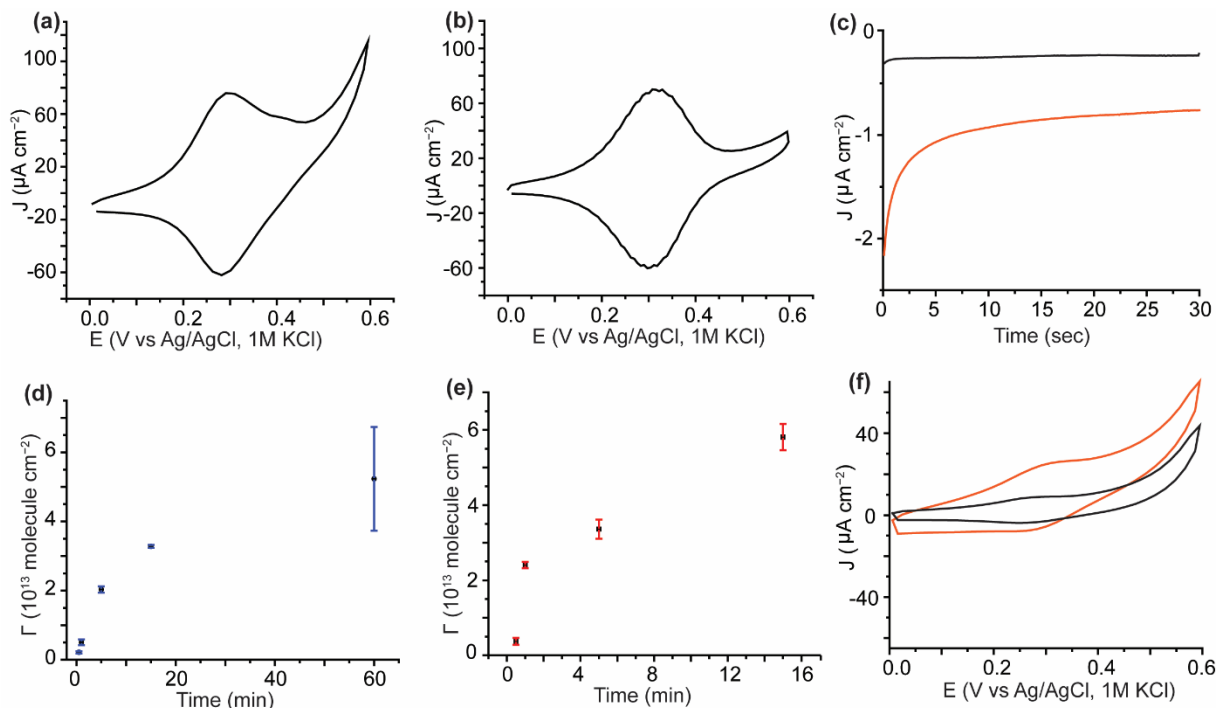| Substrate	Molecule	Preparation	Time (h)	Potential (V)	Γ(10^{13} molecule cm^{-2})
Si−H	2	spontaneous	1	None	5.2±1.5
Si−H	2	electrochemical	0.25	−0.8	5.9±0.3
Au	2	spontaneous	3	None	5.6±0.8
Au	2	spontaneous	24	None	10.2±0.2

Figure 4. CVs of **2** on p-type highly doped Si (111)−H. a) CV for a SAM of **2** grafted on Si by the spontaneous grafting method for 1 hour with a scan rate of 1 Vs^{-1}. b) CV for a SAM of **2** grafted on Si electrochemically at −0.8V for 15 min, with a scan rate of 1 Vs^{-1}. c) Chronoamperometric current for the grafting of **2** electrochemically at two different applied potentials,−0.8V (black) and −0.9V (orange) for 30 seconds. (d) Surface coverage as a function of time for **2** grafted to Si electrode spontaneously at different times. e) Surface coverage as a function of time for **2** grafted to Si electrode electrochemically at −0.8V at different times. f) CV from monolayers formed by applying −0.8V (black) with a coverage of 9.5±0.8×10^{11} molecule cm^{-2} and −0.9V (orange) with a coverage of 3.6±0.2×10^{12} for 30 seconds showing that a more negative applied potential led to more amperometric current in (c) and consequently more molecular coverage.

Apart from p-type highly doped Si (111), a solution of **2** enabled forming a monolayer on both n-type highly doped Si(111) and p-type lowly doped Si(111) (Figure S10), suggesting that the SAM formation process is independent of doping type and concentration. Table 1 shows that the surface coverage is controlled by time and potential, and highlights the difference in the grafting reaction kinetics between Si and Au. Spontaneous grafting on Si at ambient conditions enabled achieving a surface coverage of 5.2±1.5 ×10^{13} molecule cm^{-2} and this is the maximum surface coverage obtained even after increasing the grafting time to 24 hours. On the other hand, electrochemical reduction accelerates the reaction and enables the formation of a SAM with a surface coverage of 5.9±0.3×10^{13} molecule cm^{-2} in only 15 minutes The reason for the relatively lower maximum coverage in the spontaneous grafting can be attributed to the local oxidation of Si occupying some sites on the surface, whereas in electrochemical reduction, less oxide is generated. This is consistent with the large variation in the molecular coverage of the spontaneously formed SAMs versus those formed electrochemically (Figure 4d and 4e). This is also consistent with the observation of more local oxide by AFM (observed as spots) for the spontaneous grafting method.

In contrast, SAMs of **2** on Au electrode needs at least 3 hours to reach a comparable coverage to that obtained on Si in 1 hour (5.6±0.8 ×10^{13} molecule cm^{-2}). However, leaving an Au surface in the disulfide solution for 24 hours leads to ~ 40% higher coverage (10.2±0.2×10^{13} molecule cm^{-2}) than the maximum obtained on Si, and that is probably due to the different mechanism of spontaneous SAM formation of disulfides on Au that requires no oxidation of the surface,[53, 55] and therefore has more unoccupied surface sites for the molecules to assemble on.

3.4 Conversion of thiols to disulfides. It has been demonstrated that alkane thiol solutions, in deoxygenated solvents form poor quality SAMs on Si−H at very low coverage, whereas thiol solutions exposed to ambient oxygen form SAMs on Si−H within 24 hours timescale.[49] Thiols can be oxidized to disulfides in solution,[77, 78] but not known to be able to form SAMs on Si, and here we demonstrate this process, using Fourier-transform infrared spectroscopy (FTIR), by exposing the linear-alkane thiol **3** to varying amounts of oxygen. First, Figure 5a shows FTIR spectra for the disulfide **2** and the thiol **3**. Peaks observed at 480–550 cm^{-1} are assigned to the S−S stretch of **2** and are absent in the spectrum of a freshly prepared solution of **3**. Instead, the spectrum of **3** manifests the S−H stretching frequency at 2570 cm^{-1}. Figure 5b shows that exposure of the thiol solution to ambient air for 24 hours leads to the near-complete conversion of **3** to its disulfide, as evidenced by the appearance of a S−S signal between 480-550 cm^{-1} and the disappearance of the S−H signal at 2570 cm^{-1}.[79] Further bubbling of O$_2$ for 1 hour led to the loss of the disulfide signal and the appearance of absorption at 1070 cm^{-1} characteristic of =S=O species (Figure 5b). The sharp peak in the FTIR spectrum of **2** is assigned to the C=O stretching present in this ester molecule, consistent with that observed in Nikolić et al.[80] The region between 700 and
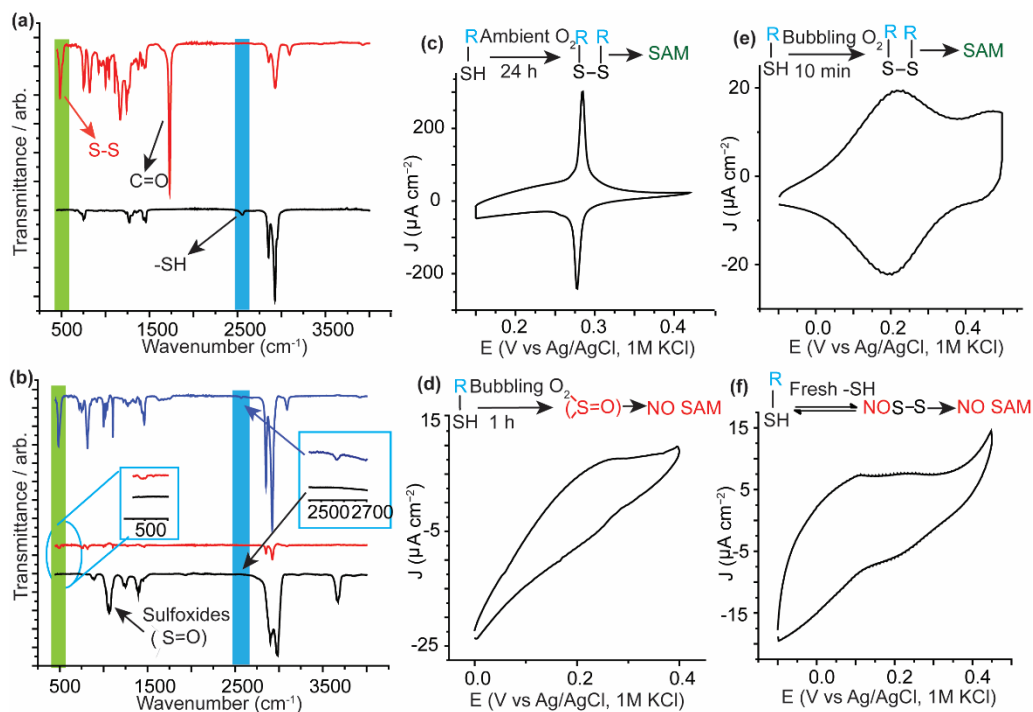
Figure 5. FTIR spectra for disulfide and thiol solutions under different oxygen conditions, and CV for a SAM of **3** with different oxygen conditions (a) The difference between disulfides and thiols solutions, with red depicting the IR spectrum of the dithiolane **2**, and black depicting the IR spectrum of the freshly prepared thiol **3**. (b) IR spectrum of a thiol solution of **3**, exposed to ambient air (blue trace), bubbled with oxygen 1 hour (black trace), and bubbled with oxygen for 10 minutes (red trace). The green band indicates the position of S−S stretching and the blue band indicates the position of SH stretching. c) CV, at 50 mVs^{-1}, for **3** pre-exposed to ambient air for 24 hours then grafted spontaneously to Si(111)−H electrode for a duration of 1 hour, d) CV, at 50 mVs^{-1}, for **3** bubbled with O$_2$ for 1 hour then grafted spontaneously to Si(111)−H electrode. (e) CV, at 50 mVs^{-1}, for **3** bubbled with O$_2$ for 10 minutes, then grafted spontaneously to Si(111)−H electrode. (f) CV, at 50 mVs^{-1}, for **3** freshly prepared and saturated with Ar gas for 1 hour then grafted spontaneously to Si(111)−H electrode.

1500 cm^{-1} is attributed to the C−C and C−H stretching and bending modes.

Consistent with FTIR measurements, exposing a thiol solution of **3** to air for 24 hours showed high coverages of ferrocene molecules in cyclic voltammetry, indicating a high density monolayer (Figure 5c). However, bubbling oxygen for 1 hour showed no ferrocene signals (Figure 5d). Excess oxygen (bubbling for 1 hour) leads to the formation of sulfoxide species that are not capable of forming a monolayer. Only when bubbling O$_2$ was reduced to 10 minutes, ferrocene signals were obtained but at a slightly lower coverage (Figure 5e).

However, a freshly prepared solution of **3** bubbled with Ar for 1 hour did not show a ferrocene signal (Figure 5f) suggesting that absence of oxygen inhibits the SAM formation. Therefore, we conclude here that exposing the thiol solution to ambient air for a duration sufficient for a conversion to disulfide enabled the formation of a complete SAM within 1 hour, in contrast to fresh thiols which needed 24 hours to form a complete monolayer at ambient conditions.[49]

3.5 SAMs on silicon versus SAMs on gold. For the purpose of comparison with standard electrodes that are typically used with thiols and disulfides, a SAM of **2** was assembled onto an Au electrode (Figure 6a). Figure 6b and 6c show CV waves, at the same scan rate, for a SAM of **2** spontaneously and electrochemically grafted onto the Au electrode, respectively. The kinetics of SAMs formed on Au is investigated by calculating the surface coverage at different spontaneous grafting times (Figure
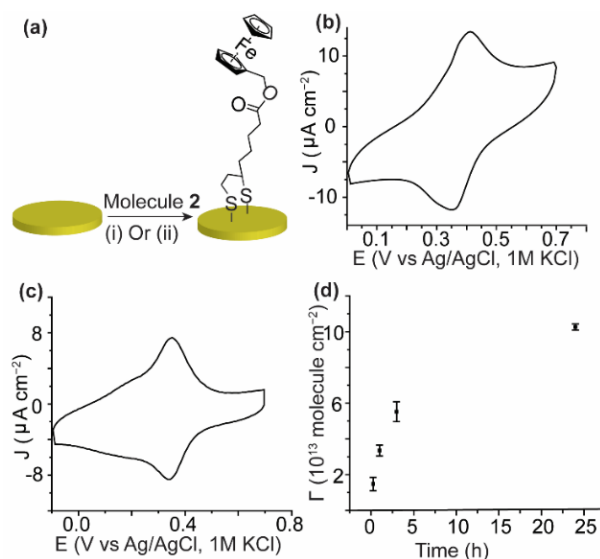

Figure 6. SAM formation of **2** on Au electrode. a) Reaction schemes for a SAM of **2** on Au b) CV at a scan rate of 1 Vs^{-1} for **2** grafted on Au by spontaneous grafting method for 3 hours. c) CV at scan rate of 1 Vs^{-1} for a SAM of **2** grafted electrochemically to Au electrode at −0.8V for 15 minutes. d) Surface coverage as a function of time for a SAM of **2** grafted on Au electrode spontaneously.
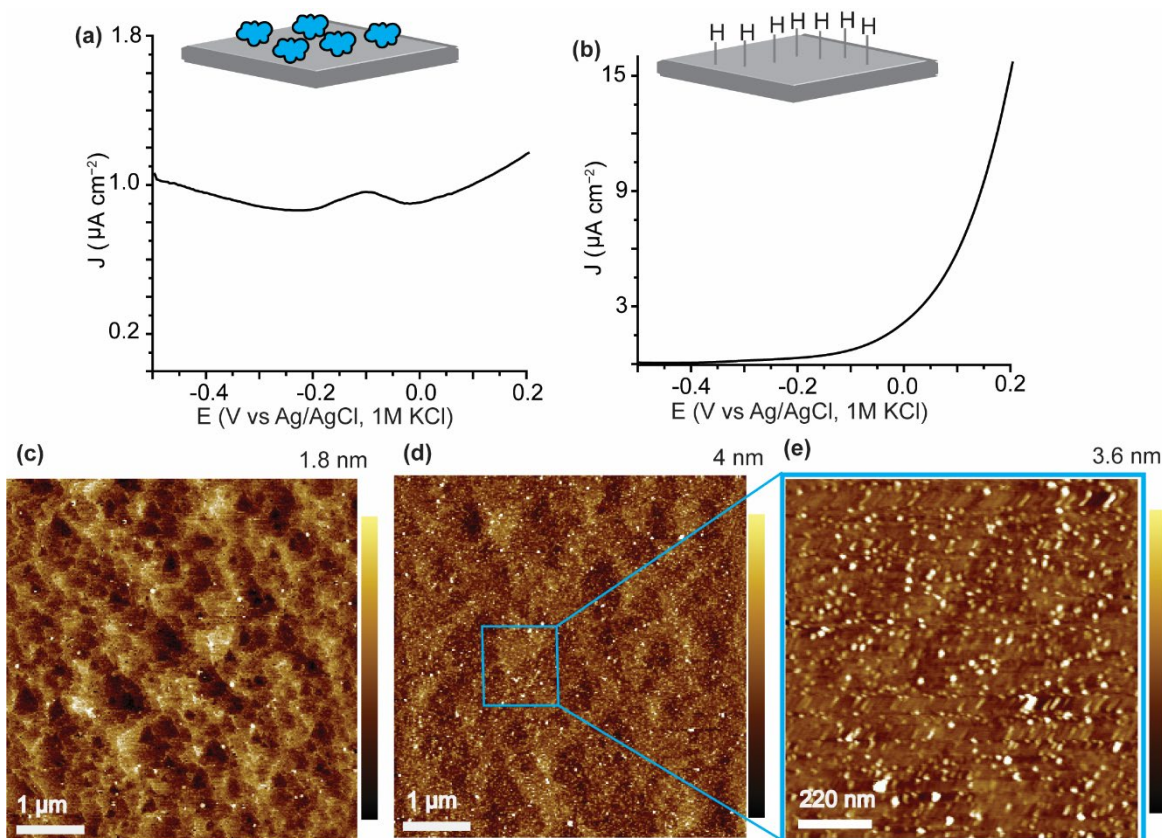
Figure 7 Formation of azurin monolayer on Si−H. a) Square wave voltammogram for a monolayer of azurin , **4**, assembled to p-type highly doped Si(111)−H surface by spontaneous grafting for 1 hour, showing a redox peak, centred at −0.1V vs Ag/AgCl reference electrode, in ammonium acetate buffer (100 mM, pH=4.6), for the copper centre in azurin. b) Square wave voltammogram for Si−H electrode incubated in ammonium acetate buffer (100 mM, pH=4.6) for 1 hour c) AFM topography image for Si−H surface in ammonium acetate buffer for 1 hour, showing clear Si terraces with few local oxide spots. d) and e) are AFM topography images for Si−H electrode after azurin grafting in ammonium acetate buffer for 1 hour.

6d). Compared to Si, Au needed longer time to form a SAM, approximately 3 hours to reach a comparable surface coverage to that achieved on Si in just 1 hour.

3.6 Electron transfer kinetics. Compared to Au, electrochemical measurements of SAMs formed from **2** on Si showed similar adsorption process with current increasing linearly with scan rate (Figure S11a, 11b and 11c). The position of the voltammetric waves , of a SAM of **2** on Si, are shifted with increasing scan rates and electron transfer rate constant (k_{et}) values were calculated using Laviron method,[81, 82] and k_{et} fitting parameters are shown in Figure S12-S13.

Most importantly, the k_{et} value of **2** on Si−H ca. 180±12 s^{-1}, only one third of those obtained for the same molecule on Au electrodes which ca. 471±24 s^{-1} (Figure S13), suggesting that Si−S contact in a monolayer platform is as conductive as that formed on Au. Therefore, disulfide monolayers on Si could prove useful in molecular electronic devices based on SAMs.

3.7 Protein azurin on Si. In addition to functionalizing surfaces and possibly nanoparticles, direct reduction of disulfide bonds on Si electrodes can be utilized to wire proteins to Si. As a prove of concept, we grafted the redox protein azurin, that has a disulfide bond at one terminal and a copper metal centre which is located inside the protein at the opposite side to the disulfide bond.[83] The square wave voltammogram show a peak with a

redox potential of −0.1 V (Figure 7a). The low peak intensity is typical of dense monolayers of azurin directly assembled on bare Au electrodes without a hydrophobic monolayer that is necessary to connect/penetrate the protein structure to the copper center.

This is ascribed to the location of the copper centre being far from the electrode and buried inside the protein matrix.[84] Square wave voltammogram of bare Si−H electrode did not show any redox peaks but rather a sharp increase in the current reflecting significant Si oxidation in the absence of the protein monolayer (Figure 7b).

The assembly of azurin was also visually assessed using AFM topography imaging which showed a packed monolayer of azurin when the Si surface is incubated in the azurin solution for 1 hour (Figure 7c and 7d). The size of the azurin spots is about 20 nm, similar to what was reported for monolayers of azurin on Au[85] and the Si(111) terraces are completely covered by azurin. In contrast, Si−H surfaces left resting in the same buffer solution and for the same incubation time (1 hour) showed clear uncovered Si(111) terraces (Figure 7e) with presence of few local oxidation spots (Figure 7c).

4. Conclusions

We have demonstrated the reduction of disulfide bonds on Si−H electrodes both spontaneously and electrochemically. Of particular note, the spontaneous grafting method involves only very mild reaction conditions consistent with operations in industrial silicon-chip manufacturing plants. The spontaneous reductive grafting process is guided by traces of water generating local nanoscale oxidation of the Si surface. Full monolayers are achieved within 1 hour, without any external catalysis. The grafting of disulfides shows significantly faster reaction kinetics on Si−H than on the typical Au electrodes. Electrochemical gating accelerates the grafting and enables a complete monolayer within 15 minutes. Further, dilute solutions of alkyl thiols, widely used to form SAMs on Au, can be used to form monolayers rapidly on Si but need to be first oxidized to linear disulfides. Similarly, we show complete monolayer formation of azurin on Si during a period of 1 hour. Electron transfer rate constants of SAMs formed on Si is comparable to that formed on Au, suggesting that thiol SAMs that have been long used on Au for (bio)electronic and electrochemical applications, can also be implemented on semiconducting Si platforms with minimal change in the conductivity of the monolayer–electrode interface. For example, electron transport of proteins on gold electrodes has been studied via anchoring protein disulfide bonds to Au electrodes.[86] The disulfide spontaneous and electrochemical reduction, reported here, offers new chemical plugs for wiring proteins to semiconducting Si for bioelectronics applications.

ASSOCIATED CONTENT

Supporting Information file in PDF format is available free of charge on the ACS Publications.

AUTHOR INFORMATION

Corresponding Author

Nadim Darwish ─ School of Molecular and Life Sciences, Curtin Institute of Functional molecules and Interfaces, Curtin University, Bentley, WA 6102, Australia

Email: nadim.darwish@curtin.edu.au.

Author Contributions

E.M.D. performed all the surface preparation, AFM imaging, and electrochemical experiments and analyzed the data. A.L.B. performed the XRR measurements .V.R.G. performed the XPS measurements and S.C. helped in XPS data fitting and analysis. Y.B.V helped with electron transfer kinetics analysis. C.R.P. helped with AFM imaging. N.D. conceived the project. E.M.D. and N.D. wrote the manuscript with contributions from other authors. All authors discussed and interpreted the results and gave approval to the final version of the manuscript.

Notes
The authors declare no conflict of interest.

ACKNOWLEDGMENT

5. References

1. Onclin, S.; Ravoo, B. J.; Reinhoudt, D. N., Engineering Silicon Oxide Surfaces Using Self-Assembled Monolayers. *Angew. Chem., Int. Ed.* **2005,** *44* (39), 6282-6304.

2. Rakshit, T.; Liang, G.-C.; Ghosh, A. W.; Datta, S., Silicon-based Molecular Electronics. *Nano Lett.* **2004,** *4* (10), 1803-1807.

3. See, P.; Paul, D. J.; Hollander, B.; Mantl, S.; Zozoulenko, I. V.; Berggren, K., High performance Si/Si/sub 1-x/Gex resonant tunneling diodes. *IEEE Electron Device Lett.* **2001,** *22* (4), 182-184.

4. Sieval, A. B.; Linke, R.; Zuilhof, H.; Sudhölter, E. J. R., High-Quality Alkyl Monolayers on Silicon Surfaces. *Adv. Mater.* **2000,** *12* (19), 1457-1460.

5. Vezzoli, A.; Brooke, R. J.; Ferri, N.; Brooke, C.; Higgins, S. J.; Schwarzacher, W.; Nichols, R. J., Charge transport at a molecular GaAs nanoscale junction. *Faraday Discuss.* **2018,** *210* (0), 397-408.

6. Vezzoli, A.; Brooke, R. J.; Ferri, N.; Higgins, S. J.; Schwarzacher, W.; Nichols, R. J., Single-Molecule Transport at a Rectifying GaAs Contact. *Nano Lett.* **2017,** *17* (2), 1109-1115.

7. Aragonès, A. C.; Darwish, N.; Ciampi, S.; Sanz, F.; Gooding, J. J.; Díez-Pérez, I., Single-molecule electrical contacts on silicon electrodes under ambient conditions. *Nat. Commun.* **2017,** *8* (1), 1-8.

8. Li, Y.; Calder, S.; Yaffe, O.; Cahen, D.; Haick, H.; Kronik, L.; Zuilhof, H., Hybrids of Organic Molecules and Flat, Oxide-Free Silicon: High-Density Monolayers, Electronic Properties, and Functionalization. *Langmuir* **2012,** *28* (26), 9920-9929.

9. Gooding, J. J.; Mearns, F.; Yang, W.; Liu, J., Self-Assembled Monolayers into the 21st Century: Recent Advances and Applications. *Electroanalysis* **2003,** *15* (2), 81-96.

10. Aswal, D. K.; Lenfant, S.; Guerin, D.; Yakhmi, J. V.; Vuillaume, D., Self assembled monolayers on silicon for molecular electronics. *Anal. Chim. Acta.* **2006,** *568* (1-2), 84-108.

11. Sieval, A. B.; Demirel, A. L.; Nissink, J. W. M.; Linford, M. R.; van der Maas, J. H.; de Jeu, W. H.; Zuilhof, H.; Sudhölter, E. J. R., Highly Stable Si−C Linked Functionalized Monolayers on the Silicon (100) Surface. *Langmuir* **1998,** *14* (7), 1759-1768.

12. Darwish, N.; Eggers, P. K.; Ciampi, S.; Tong, Y.; Ye, S.; Paddon-Row, M. N.; Gooding, J. J., Probing the effect of the solution environment around redox-active moieties using rigid anthraquinone terminated

molecular rulers. *J. Am. Chem. Soc.* **2012,** *134* (44), 18401-18409.

13. Darwish, N.; Paddon-Row, M. N.; Gooding, J. J., Surface-Bound Norbornylogous Bridges as Molecular Rulers for Investigating Interfacial Electrochemistry and as Single Molecule Switches. *Acc. Chem. Res.* **2014,** *47* (2), 385-395.

14. Darwish, N.; Aragonès, A. C.; Darwish, T.; Ciampi, S.; Diez-Perez, I., Multi-responsive photo-and chemo-electrical single-molecule switches. *Nano Lett.* **2014,** *14* (12), 7064-7070.

15. Wang, J.; Zhou, Y.; Watkinson, M.; Gautrot, J.; Krause, S., High-sensitivity light-addressable potentiometric sensors using silicon on sapphire functionalized with self-assembled organic monolayers. *Sens. Actuators, B* **2015,** *209*, 230-236.

16. Zhao, C.; Brinkhoff, T.; Burchardt, M.; Simon, M.; Wittstock, G., Surface selection, adhesion, and retention behavior of marine bacteria on synthetic organic surfaces using self-assembled monolayers and atomic force microscopy. *Ocean Dynamics* **2009,** *59* (2), 305-315.

17. Alharbi, A. R. M.; Andersson, J. M.; Köper, I.; Andersson, G. G., Investigating the Structure of Self-Assembled Monolayers Related to Biological Cell Membranes. *Langmuir* **2019,** *35* (44), 14213-14221.

18. Murray, D. J.; Kim, J. H.; Grzincic, E. M.; Kim, S. C.; Abate, A. R.; Zuckermann, R. N., Uniform, Large-Area, Highly Ordered Peptoid Monolayer and Bilayer Films for Sensing Applications. *Langmuir* **2019,** *35* (42), 13671-13680.

19. Robertson, E. J.; Nehls, E. M.; Zuckermann, R. N., Structure–Rheology Relationship in Nanosheet-Forming Peptoid Monolayers. *Langmuir* **2016,** *32* (46), 12146-12158.

20. Nuzzo, R. G.; Allara, D. L., Adsorption of bifunctional organic disulfides on gold surfaces. *J. Am. Chem. Soc.* **1983,** *105* (13), 4481-4483.

21. Ulman, A., Formation and Structure of Self-Assembled Monolayers. *Chem. Rev.* **1996,** *96* (4), 1533-1554.

22. Aragonès, A. C.; Darwish, N.; Im, J.; Lim, B.; Choi, J.; Koo, S.; Díez-Pérez, I., Fine-Tuning of Single-Molecule Conductance by Tweaking Both Electronic Structure and Conformation of Side Substituents. *Chem. - Eur. J.* **2015,** *21* (21), 7716-7720.

23. Reimers, J. R.; Wang, Y.; Cankurtaran, B. O.; Ford, M. J., Chemical Analysis of the Superatom Model for Sulfur-Stabilized Gold Nanoparticles. *J. Am. Chem. Soc.* **2010,** *132* (24), 8378-8384.

24. Chi, Q.; Ford, M. J.; Halder, A.; Hush, N. S.; Reimers, J. R.; Ulstrup, J., Sulfur ligand mediated electrochemistry of gold surfaces and nanoparticles: What, how, and why. *Curr. Opin. Electrochem.* **2017,** *1* (1), 7-15.

25. Reimers, J. R.; Ford, M. J.; Halder, A.; Ulstrup, J.; Hush, N. S., Gold surfaces and nanoparticles are protected by Au(0)-thiyl species and are destroyed when Au(I)-thiolates form. *Proc. Natl. Acad. Sci. U.S.A.* **2016,** *113* (11), E1424-E1433.

26. Yan, J.; Ouyang, R.; Jensen, P. S.; Ascic, E.; Tanner, D.; Mao, B.; Zhang, J.; Tang, C.; Hush, N. S.; Ulstrup, J.; Reimers, J. R., Controlling the Stereochemistry and Regularity of Butanethiol Self-Assembled Monolayers on Au(111). *J. Am. Chem. Soc.* **2014,** *136* (49), 17087-17094.

27. Qiu, X.; Ivasyshyn, V.; Qiu, L.; Enache, M.; Dong, J.; Rousseva, S.; Portale, G.; Stöhr, M.; Hummelen, J. C.; Chiechi, R. C., Thiol-free self-assembled oligoethylene glycols enable robust air-stable molecular electronics. *Nat. Mater.* **2020,** *19* (3), 330-337.

28. Mani, G.; Johnson, D. M.; Marton, D.; Dougherty, V. L.; Feldman, M. D.; Patel, D.; Ayon, A. A.; Agrawal, C. M., Stability of Self-Assembled Monolayers on Titanium and Gold. *Langmuir* **2008,** *24* (13), 6774-6784.

29. Halik, M.; Hirsch, A., The Potential of Molecular Self-Assembled Monolayers in Organic Electronic Devices. *Adv. Mater.* **2011,** *23*, 2689-95.

30. Linford, M. R.; Chidsey, C. E. D., Alkyl monolayers covalently bonded to silicon surfaces. *J. Am. Chem. Soc.* **1993,** *115* (26), 12631-12632.

31. Gooding, J. J.; Ciampi, S., The molecular level modification of surfaces: from self-assembled monolayers to complex molecular assemblies. *Chem. Soc. Rev.* **2011,** *40* (5), 2704-18.

32. Ciampi, S.; Böcking, T.; Kilian, K. A.; James, M.; Harper, J. B.; Gooding, J. J., Functionalization of Acetylene-Terminated Monolayers on Si(100) Surfaces: A Click Chemistry Approach. *Langmuir* **2007,** *23* (18), 9320-9329.

33. Buriak, J. M., Illuminating Silicon Surface Hydrosilylation: An Unexpected Plurality of Mechanisms. *Chem. Mater.* **2014,** *26* (1), 763-772.

34. Stewart, M. P.; Robins, E. G.; Geders, T. W.; Allen, M. J.; Cheul Choi, H.; Buriak, J. M., Three Methods for Stabilization and Functionalization of Porous Silicon Surfaces via Hydrosilylation and

Electrografting Reactions. *Phys. Status Solidi A* **2000,** *182* (1), 109-115.

35. Sun, Q. Y.; de Smet, L. C.; van Lagen, B.; Wright, A.; Zuilhof, H.; Sudholter, E. J., Covalently attached monolayers on hydrogen-terminated Si(100): extremely mild attachment by visible light. *Angew. Chem., Int. Ed. Engl.* **2004,** *43* (11), 1352-5.

36. Thissen, P.; Seitz, O.; Chabal, Y. J., Wet chemical surface functionalization of oxide-free silicon. *Prog. Surf. Sci.* **2012,** *87* (9), 272-290.

37. Ciampi, S.; Harper, J. B.; Gooding, J. J., Wet chemical routes to the assembly of organic monolayers on silicon surfaces via the formation of Si-C bonds: surface preparation, passivation and functionalization. *Chem. Soc. Rev.* **2010,** *39* (6), 2158-83.

38. Sieval, A. B.; Opitz, R.; Maas, H. P. A.; Schoeman, M. G.; Meijer, G.; Vergeldt, F. J.; Zuilhof, H.; Sudhölter, E. J. R., Monolayers of 1-Alkynes on the H-Terminated Si(100) Surface. *Langmuir* **2000,** *16* (26), 10359-10368.

39. Sun, J.; Deng, L., Cobalt Complex-Catalyzed Hydrosilylation of Alkenes and Alkynes. *ACS Catal.* **2016,** *6* (1), 290-300.

40. Boukherroub, R.; Wayner, D. D. M., Controlled Functionalization and Multistep Chemical Manipulation of Covalently Modified Si(111) Surfaces1. *J. Am. Chem. Soc.* **1999,** *121* (49), 11513-11515.

41. Boukherroub, R.; Morin, S.; Bensebaa, F.; Wayner, D. D. M., New Synthetic Routes to Alkyl Monolayers on the Si(111) Surface1. *Langmuir* **1999,** *15* (11), 3831-3835.

42. van den Boom, A. F. J.; Pujari, S. P.; Bannani, F.; Driss, H.; Zuilhof, H., Fast room-temperature functionalization of silicon nanoparticles using alkyl silanols. *Faraday Discuss.* **2020,** *222* (0), 82-94.

43. Escorihuela, J.; Zuilhof, H., Rapid Surface Functionalization of Hydrogen-Terminated Silicon by Alkyl Silanols. *J. Am. Chem. Soc.* **2017,** *139* (16), 5870-5876.

44. Fabre, B., Ferrocene-Terminated Monolayers Covalently Bound to Hydrogen-Terminated Silicon Surfaces. Toward the Development of Charge Storage and Communication Devices. *Acc. Chem. Res.* **2010,** *43* (12), 1509-1518.

45. Fabre, B., Functionalization of Oxide-Free Silicon Surfaces with Redox-Active Assemblies. *Chem. Rev.* **2016,** *116* (8), 4808-4849.

46. Hu, M.; Hauger, T. C.; Olsen, B. C.; Luber, E. J.; Buriak, J. M., UV-Initiated Si–S, Si–Se, and Si–Te Bond Formation on Si(111): Coverage, Mechanism, and Electronics. *J. Phys. Chem. C* **2018,** *122* (25), 13803-13814.

47. Buriak, J. M.; Sikder, M. D. H., From Molecules to Surfaces: Radical-Based Mechanisms of Si–S and Si–Se Bond Formation on Silicon. *J. Am. Chem. Soc.* **2015,** *137* (30), 9730-9738.

48. Sano, H.; Ohno, K.; Ichii, T.; Murase, K.; Sugimura, H., Alkanethiol Self-Assembled Monolayers Formed on Silicon Substrates. *Jpn. J. Appl. Phys.* **2010,** *49*.

49. Peiris, C. R.; Ciampi, S.; Dief, E. M.; Zhang, J.; Canfield, P. J.; Le Brun, A. P.; Kosov, D. S.; Reimers, J. R.; Darwish, N., Spontaneous S–Si bonding of alkanethiols to Si(111)–H: towards Si–molecule–Si circuits. *Chem. Sci.* **2020,** *11* (20), 5246-5256.

50. Karimi, M.; Ignasiak, M. T.; Chan, B.; Croft, A. K.; Radom, L.; Schiesser, C. H.; Pattison, D. I.; Davies, M. J., Reactivity of disulfide bonds is markedly affected by structure and environment: implications for protein modification and stability. *Sci. Rep.* **2016,** *6* (1), 38572.

51. Packer, L.; Witt, E. H.; Tritschler, H. J., alpha-Lipoic acid as a biological antioxidant. *Free Radicals Biol. Med.* **1995,** *19* (2), 227-50.

52. Rochette, L.; Ghibu, S.; Richard, C.; Zeller, M.; Cottin, Y.; Vergely, C., Direct and indirect antioxidant properties of α-lipoic acid and therapeutic potential. *Mol. Nutr. Food Res.* **2013,** *57* (1), 114-25.

53. Lavrich, D. J.; Wetterer, S. M.; Bernasek, S. L.; Scoles, G., Physisorption and Chemisorption of Alkanethiols and Alkyl Sulfides on Au(111). *J. Phys. Chem. B* **1998,** *102* (18), 3456-3465.

54. Love, J. C.; Estroff, L. A.; Kriebel, J. K.; Nuzzo, R. G.; Whitesides, G. M., Self-Assembled Monolayers of Thiolates on Metals as a Form of Nanotechnology. *Chem. Rev.* **2005,** *105* (4), 1103-1170.

55. Bain, C. D.; Biebuyck, H. A.; Whitesides, G. M., Comparison of self-assembled monolayers on gold: coadsorption of thiols and disulfides. *Langmuir* **1989,** *5* (3), 723-727.

56. Vericat, C.; Vela, M. E.; Benitez, G.; Carro, P.; Salvarezza, R. C., Self-assembled monolayers of thiols and dithiols on gold: new challenges for a well-known system. *Chem. Soc. Rev.* **2010,** *39* (5), 1805-34.

57. Dilimon, V. S.; Rajalingam, S.; Delhalle, J.; Mekhalif, Z., Self-assembly mechanism of thiol, dithiol, dithiocarboxylic acid, disulfide and diselenide on gold: an electrochemical impedance study. *Phys. Chem. Chem. Phys.* **2013,** *15* (39), 16648-16656.

58.   Tang, H.; Tsarevsky, N. V., Lipoates as building blocks of sulfur-containing branched macromolecules. *Polym. Chem.* **2015,** *6* (39), 6936-6945.

59.   Vericat, C.; Vela, M. E.; Corthey, G.; Pensa, E.; Cortés, E.; Fonticelli, M. H.; Ibañez, F.; Benitez, G. E.; Carro, P.; Salvarezza, R. C., Self-assembled monolayers of thiolates on metals: a review article on sulfur-metal chemistry and surface structures. *RSC Adv.* **2014,** *4* (53), 27730-27754.

60.   Sahli, R.; Fave, C.; Raouafi, N.; Boujlel, K.; Schollhorn, B.; Limoges, B., Switching on/off the chemisorption of thioctic-based self-assembled monolayers on gold by applying a moderate cathodic/anodic potential. *Langmuir* **2013,** *29* (17), 5360-8.

61.   Kumar, S.; Soni, S.; Danowski, W.; van Beek, C. L. F.; Feringa, B. L.; Rudolf, P.; Chiechi, R. C., Correlating the Influence of Disulfides in Monolayers across Photoelectron Spectroscopy Wettability and Tunneling Charge-Transport. *J. Am. Chem. Soc.* **2020,** *142* (35), 15075-15083.

62.   Sahli, R.; Fave, C.; Raouafi, N.; Boujlel, K.; Schöllhorn, B.; Limoges, B., Switching On/Off the Chemisorption of Thioctic-Based Self-Assembled Monolayers on Gold by Applying a Moderate Cathodic/Anodic Potential. *Langmuir* **2013,** *29* (17), 5360-5368.

63.   Berner, S.; Lidbaum, H.; Ledung, G.; Åhlund, J.; Nilson, K.; Schiessling, J.; Gelius, U.; Bäckvall, J.-E.; Puglia, C.; Oscarsson, S., Electronic and structural studies of immobilized thiol-derivatized cobalt porphyrins on gold surfaces. *Appl. Surf. Sci.* **2007,** *253*, 7540-7548.

64.   Yubero, F.; Holgado, J. P.; Barranco, A.; González-Elipe, A. R., Determination of surface nanostructure from analysis of electron plasmon losses in XPS. *Surf. Interface Anal.* **2002,** *34* (1), 201-205.

65.   Ong, C. W.; Huang, H.; Zheng, B.; Kwok, R. W. M.; Hui, Y. Y.; Lau, W. M., X-ray photoemission spectroscopy of nonmetallic materials: Electronic structures of boron and BxOy. *J. Appl. Phys.* **2004,** *95* (7), 3527-3534.

66.   Deng, W.; Fujita, D.; Yang, L.; Nejo, H.; Bai, C.-L., Multilayer Formation of Copper Ions (Cu2+) Deposited onto Self-Assembled Monolayers of Alkanedithiols on Au (111) Surfaces. *Jpn. J. Appl. Phys.* **2000,** *39*.

67.   Laibinis, P. E.; Whitesides, G. M., Self-assembled monolayers of n-alkanethiolates on copper are barrier films that protect the metal against oxidation by air. *J. Am. Chem. Soc.* **1992,** *114* (23), 9022-9028.

68.   Hassan, F. M.; Batmaz, R.; Li, J.; Wang, X.; Xiao, X.; Yu, A.; Chen, Z., Evidence of covalent synergy in silicon–sulfur–graphene yielding highly efficient and long-life lithium-ion batteries. *Nat. Commun.* **2015,** *6* (1), 8597.

69.   Checco, A.; Schollmeyer, H.; Daillant, J.; Guenoun, P.; Boukherroub, R., Nanoscale Wettability of Self-Assembled Monolayers Investigated by Noncontact Atomic Force Microscopy. *Langmuir* **2006,** *22* (1), 116-126.

70.   Rahpeima, S.; Dief, E. M.; Peiris, C. R.; Ferrie, S.; Duan, A.; Ciampi, S.; Raston, C. L.; Darwish, N., Reduced graphene oxide–silicon interface involving direct Si–O bonding as a conductive and mechanical stable ohmic contact. *Chem. Commun.* **2020,** *56* (46), 6209-6212.

71.   Neises, B.; Steglich, W., Simple Method for the Esterification of Carboxylic Acids. *Angew. Chem., Int. Ed. Engl.* **1978,** *17* (7), 522-524.

72.   Wayner, D. D. M.; Wolkow, R. A., Organic modification of hydrogen terminated silicon surfaces1. *J. Chem. Soc., Perkin Trans. 2* **2002,** (1), 23-34.

73.   Antonello, S.; Benassi, R.; Gavioli, G.; Taddei, F.; Maran, F., Theoretical and Electrochemical Analysis of Dissociative Electron Transfers Proceeding through Formation of Loose Radical Anion Species: Reduction of Symmetrical and Unsymmetrical Disulfides. *J. Am. Chem. Soc.* **2002,** *124* (25), 7529-7538.

74.   Moo, C. S.; Ng, K. S.; Chen, Y. P.; Hsieh, Y. C. In *State-of-Charge Estimation with Open-Circuit-Voltage for Lead-Acid Batteries*, 2007 Power Conversion Conference - Nagoya, 2-5 April 2007; 2007; pp 758-762.

75.   Okorn-Schmidt, H. F., Characterization of silicon surface preparation processes for advanced gate dielectrics. *IBM J. Res. Dev.* **1999,** *43* (3), 351-326.

76.   Goldin, M. M.; Kolesnikov, V. A.; Khubutiya, M. S.; Volkov, A. G.; Blanchard, G. J.; Evseev, A. K.; Goldin, M. M., Open circuit potential shifts of activated carbon in aqueous solutions during chemical and adsorption interactions. *J. Appl. Electrochem.* **2008,** *38* (10), 1369-1374.

77.   Bagi, N.; Kaizer, J.; Speier, G., Oxidation of thiols to disulfides by dioxygen catalyzed by a bioinspired organocatalyst. *RSC Adv.* **2015,** *5* (57), 45983-45986.

78.   Ali, M. H.; McDermott, M., Oxidation of thiols to disulfides with molecular bromine on hydrated silica gel support. *Tetrahedron Lett.* **2002,** *43* (35), 6271-6273.

79.   Das, P.; Ray, S.; Bhaumik, A.; Banerjee, B.; Mukhopadhyay, C., Cubic Ag2O nanoparticle incorporated mesoporous silica with large bottle-neck like mesopores for the aerobic oxidative synthesis of disulfide. *RSC Adv.* **2015,** *5* (9), 6323-6331.

80.   Nikolić, R. S.; Krstić, N. S.; Nikolić, G. M.; Kocić, G. M.; Cakić, M. D.; Anđelković, D. H., Molecular mechanisms of beneficial effects of lipoic acid in copper intoxicated rats assessment by FTIR and ESI-MS. *Polyhedron* **2014,** *80*, 223-227.

81.   Laviron, E., General expression of the linear potential sweep voltammogram in the case of diffusionless electrochemical systems. *J. Electroanal. Chem. Interfacial Electrochem.* **1979,** *101* (1), 19-28.

82.   Laviron, E., Surface linear potential sweep voltammetry: Equation of the peaks for a reversible reaction when interactions between the adsorbed molecules are taken into account. *J. Electroanal. Chem. Interfacial Electrochem.* **1974,** *52* (3), 395-402.

83.   Bonander, N.; Leckner, J.; Guo, H.; Karlsson, B. G.; Sjölin, L., Crystal structure of the disulfide bond-deficient azurin mutant C3A/C26A. *Eur. J. Biochem.* **2000,** *267* (14), 4511-4519.

84.   Hamzehloei, A.; Zahra Bathaie, S.; Mousavi, M. F., Probing redox reaction of azurin protein immobilized on hydroxyl-terminated self-assembled monolayers with different lengths. *J. Electroanal. Chem.* **2015,** *755*, 27-38.

85.   Wu, H.; Feng, X.; Kieviet, B. D.; Zhang, K.; Zandvliet, H. J. W.; Canters, G. W.; Schön, P. M.; Vancso, G. J., Electrochemical atomic force microscopy reveals potential stimulated height changes of redox responsive Cu-azurin on gold. *Eur. Polym. J.* **2016,** *83*, 529-537.

86.   Ruiz, M. P.; Aragonès, A. C.; Camarero, N.; Vilhena, J. G.; Ortega, M.; Zotti, L. A.; Pérez, R.; Cuevas, J. C.; Gorostiza, P.; Díez-Pérez, I., Bioengineering a Single-Protein Junction. *J. Am. Chem. Soc.* **2017,** *139* (43), 15337-15346.